The Astrophysical Journal, 879:4 (8pp), 2019 July 1 https://doi.org/10.3847/1538-4357/ab2240

Repeating Fast Radio Bursts from Magnetars with Low Magnetospheric Twist

Zorawar Wadiasingh[1,2,3] and Andrey Timokhin[1,4,5]
[1] Astrophysics Science Division, NASA Goddard Space Flight Center, Greenbelt, MD 20771, USA; zwadiasingh@gmail.com
[2] Universities Space Research Association (USRA), Columbia, MD 21046, USA
[3] Centre for Space Research, North-West University, Potchefstroom, South Africa
[4] University of Maryland, College Park (UMDCP/CRESSTII), College Park, MD 20742, USA
[5] Department of Physics, The George Washington University, 725 21st St. NW, Washington, DC 20052, USA
Received 2019 April 26; revised 2019 May 13; accepted 2019 May 15; published 2019 June 26

Abstract

We analyze the statistics of pulse arrival times in fast radio burst (FRB) 121102 and demonstrate that they are remarkably similar to statistics of magnetar high-energy short bursts. Motivated by this correspondence, we propose that repeating FRBs are generated during short bursts in the closed field line zone of magnetar magnetospheres via a pulsar-like emission mechanism. Crustal slippage events dislocate field line foot points, initiating intense particle acceleration and pair production, giving rise to coherent radio emission similar to that generated near pulsar polar caps. We argue that the energetics of FRB 121102 can be readily accounted for if the efficiency of the conversion of Poynting flux into coherent radio emission is $\sim 10^{-4}$–10^{-2}; values consistent with empirical efficiencies of radio emission in pulsars and radio-loud magnetars. Such a mechanism could operate only in magnetars with preexisting low twist of the magnetosphere, so that the charge density in the closed zone is initially insufficient to screen the electric field provoked by the wiggling of magnetic field lines and is low enough to let $\sim$1 GHz radio emission escape the magnetosphere, which can explain the absence of FRBs from known magnetars. The pair cascades crowd the closed flux tubes with plasma, screening the accelerating electric field, thus limiting the radio pulse duration to $\sim$1 ms. Within the framework of our model, the current data set of the polarization angle variation in FRB 121102 suggests a magnetic obliquity $\alpha \lesssim 40^\circ$ and viewing angle ζ with respect to the spin axis $\alpha < \zeta < 180^\circ - \alpha$.

Key words: plasmas – pulsars: general – relativistic processes – stars: magnetars – stars: magnetic field – stars: neutron

1. Introduction

Fast radio bursts (FRBs) are curious phenomena with short $\sim$1–10 ms observed durations, extraordinary dispersion measures, and high brightness temperatures. Repeating FRBs[6] (Spitler et al. 2016; CHIME/FRB Collaboration et al. 2019) suggest that at least some subset of FRBs originate from nondestructive events. The repeater FRB 121102 is hitherto the most well-studied with an accurate localization and distance of $d_L \sim 1$ Gpc (Tendulkar et al. 2017), implying isotropic-equivalent burst energies $\mathcal{E}_{\rm iso} \lesssim 10^{40}$ erg. For reviews, see Katz (2018), Platts et al. (2018), and Petroff et al. (2019).

Isolated neutron stars (NSs), particularly magnetars, have been suggested as a progenitor for FRB 121102 owing to the energetics of FRBs, high magnetic fields of NSs, and flaring activity of magnetars (Popov & Postnov 2010, 2013; Lyubarsky 2014; Katz 2016; Beloborodov 2017; Lyutikov 2017, 2019; Wang et al. 2018; Metzger et al. 2019), with the radio emission site being within or external to the magnetosphere.

In this work, we advocate the view that the radio emission originates within the closed field line zone of the magnetosphere via a pulsar-like coherent emission mechanism. We motivate our model by demonstrating that FRB 121102's burst statistics bear striking similarity to short recurrent high-energy bursts of magnetars , which are generally recognized as distinct phenomena from giant flares. Quasiperiodic oscillations, associated with crustal magnetoelastic torsional oscillations, have been reported for magnetar short bursts and therefore suggest a low-altitude crustal NS quake connection to this phenomena (Huppenkothen et al. 2014a, 2014c).

NSs, including magnetars, are known to generate coherent radio emission. The generation of relativistic electron/positron pairs is generally accepted to be a necessary condition for operation of coherent radio emission in magnetospheres of NSs. In the galactic magnetar population, high-energy burst activity alters the current system in the magnetosphere and is associated both with the suppression (Archibald et al. 2017) and activation (e.g., Camilo et al. 2006, 2018) of coherent radio emission, presumably by altering electric fields and charge loading within the magnetosphere which regulates pair production along open magnetic field lines.

Persistent nonthermal soft and hard X-ray emission in known magnetars of our galaxy is thought to arise via particle acceleration along closed field lines from slow dissipation of large-scale twists in a nonpotential magnetosphere with high plasma density (e.g., Thompson et al. 2002; Baring & Harding 2007; Beloborodov & Thompson 2007; Beloborodov 2013a). For such large field twists, the transient current density is readily satisfied for any crustal dislocations imparted on magnetic foot points (FPs) in NS crust deformations. As we show in this work, below a critical value of the field twist, this charge-abundance condition is not met and large transient electric fields necessary for avalanche pair production and operation of FRBs may result. In our model, the putative driver for FRBs is identical to short bursts in galactic magnetars, namely NS crust slippages, but differentiated by the qualitative nature of the dissipation and emission set by the state of the magnetosphere.

[6] Also see Linscott & Erkes (1980).

In Section 2, we detail the observational motivation for our magnetar model from the polarization and burst statistics of FRB 121102. In Section 3, we describe our model, its self-consistency, and potential observational discriminants. A summary follows in Section 4.

2. Phenomenological Motivation from FRB 121102

2.1. Lognormality of Bursts and Power-law Fluence Distributions

Seemingly random recurrent high-energy bursts from galactic magnetars are common and a defining trait, with a broad energy range $\sim 10^{36}$–10^{42} erg. They are superficially distinct from FRBs, with T_{90} durations 0.01–1 s, i.e., $\sim$10 to 10^3 times longer than FRB pulses. Yet, although the radiative processes are dissimilar, the underlying driver may be identical by virtue of the occurrence and fluence distributions. In contrast to giant flares, there is evidence for confinement of plasma (in closed zones) rather than outflows in short bursts. The fluence range implies $\ll 10^{-3}$ fractional depletion of the $\sim 10^{46}$–10^{48} erg magnetic reservoir per burst. The high-energy spectrum of short bursts is quasithermal and may be described by a two-blackbody model (e.g., Israel et al. 2008; Lin et al. 2012; van der Horst et al. 2012; Younes et al. 2014; Collazzi et al. 2015). The two-blackbody model indicates temperatures $T_{\rm cool} \sim$ 3–5 keV and $T_{\rm hot} \sim$ 10–50 keV, with inferred cool and hot emission areas $[(0.3–1)R_*]^2$ and $[(0.03–0.1)\ R_*]^2$ (R_* the radius of the NS), respectively, with similar flux in both components. The hotter component is indicative of compactness and generally interpreted as arising from hot spots localized near magnetic field line FPs. Indeed, changes in the soft X-ray pulse profiles and surface heating are ubiquitous during such short burst episodes.

The phenomenology of short bursts is worth noting for comparison with FRB 121102. First, magnetar short bursts are episodic: intense activity with hundreds of bursts in hours may be followed by inactivity of months/years. Such episodic behavior is generally predicted by recent magnetothermal models of magnetar crustal stresses (e.g., Perna & Pons 2011; Viganò et al. 2013; Lander et al. 2015). Second, the waiting time distribution of bursts within episodes is lognormal (Hurley et al. 1994; Göğüş et al. 1999, 2000; Gavriil et al. 2004; Savchenko et al. 2010), typically with mean $\sim$100 s and width $\sim$1 dex. The waiting time of bursts may be correlated with arrival time, but generally no robust correlation exists for fluence with waiting or arrival time (Cheng et al. 1996). Moreover, evidence for a spin-phase dependence of short bursts is generally weak (e.g., Collazzi et al. 2015); the duty cycle of bursts over a spin period can be broad and weakly varying over a known rotational ephemeris. If the bursts are intrinsically beamed, strong evidence for phase dependence is not expected to emerge without significantly larger samples of bursts (Elenbaas et al. 2018) owing to the large separation of timescales between the short burst durations and long spin period. The inverse problem of establishing periodicity from burst arrivals would clearly be challenging for a limited collection of bursts. Third, the differential distribution of fluences $\mathcal{F}$ can be described by a power law $dN/d\mathcal{F} \propto \mathcal{F}^{-\gamma}$ with $\gamma \sim$ 1.4–2.0 for a multitude of burst episodes (e.g., Turolla et al. 2015, and references therein).

To date, Zhang et al. (2018; hereafter Z18) report the largest public sample of FRB 121102 bursts observed on 2017 August 26 at 4–8 GHz at the Green Bank Telescope (GBT). Z18 report no evidence of periodicity in burst arrival times. In that sample of 93 bursts spanning five hours of continuously telescope coverage, the fluence of bursts varies $\mathcal{F} \in [13, 606]$ Jy μs with standard uncertainties of $\delta\mathcal{F} \sim$ 10–15 Jy μs, with an instrumental threshold of $\sim$10–30 Jy μs. Assuming a flat spectral index over bandwidth ΔW, this implies isotropic-equivalent fluences

$$\mathcal{E}_{\rm iso} \lesssim 3 \times 10^{39} \left(\frac{\mathcal{F}}{600\ {\rm Jy}\ \mu{\rm s}}\right)\left(\frac{\Delta W}{4\ {\rm GHz}}\right)\left(\frac{d_L}{1\ {\rm Gpc}}\right)^2 \ {\rm erg}. \quad (1)$$

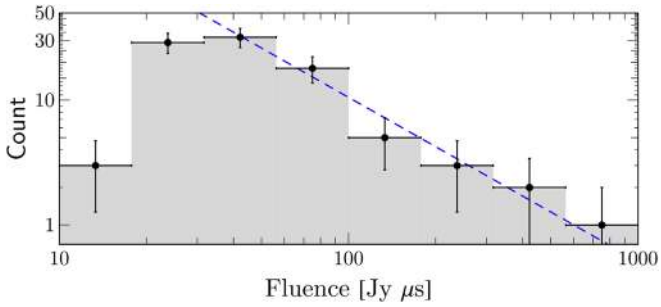

Figure 1. Histogram of fluences of bursts from FRB 121102 (with Poisson uncertainties) from Z18. The blue dash line depicts a power law $N \sim 4470\mathcal{F}^{-\gamma+1}$ with index of $\gamma = 2.3$, for $\mathcal{F} \gtrsim 30$ Jy μs.

In Figure 1, we display a coarsely binned (bin width $\gg \delta\mathcal{F}$) histogram of fluences for the Z18 sample. Kolmogorov–Smirnov (KS) and Anderson–Darling (AD) tests both strongly reject a purely exponential distribution of fluences above $\mathcal{F} > 30$ Jy μs ($p \sim 10^{-7}$–$10^{-6} \ll 0.01$), while they do not reject a power-law distribution. Above $\mathcal{F} \gtrsim 30$ Jy μs, we obtain a binned Poissonian maximum likelihood fit, $dN/d\mathcal{F} \propto \mathcal{F}^{-\gamma}$ with $\gamma \sim 2.3 \pm 0.2$. Via Monte Carlo exploration, we notice that if events are drawn from this power-law distribution, the paucity of low fluence events below $\sim$30 Jy μs is consistent with a toy model with an instrumental threshold of $\sim$10 Jy μs and $\delta\mathcal{F} \sim$ 10 Jy μs. The index $\gamma \sim 2.3$ is somewhat steeper than that for magnetar short bursts, although the limited statistics warrant a larger sample to test for any Weibull distribution-like curvature/cutoff to the power law. The steeper index of fluences may be regulated by the efficiency of the emission process or a propagation effect.

In Figure 2, the next burst waiting time ($\equiv \Delta t_i^{i+1} = t_{i+1} - t_i$) from Z18 is depicted (see also Katz 2019). There are three salient features worth highlighting. For the bulk of events where $\Delta t_i^{i+1} > 1$ s, we find that the waiting time distribution of bursts is consistent with a lognormal distribution of mean $\approx$60 s (50 s in the source frame). Second, the waiting time of bursts is correlated with arrival time as in magnetar short bursts (e.g., Cheng et al. 1996; Gavriil et al. 2004). A least squares analysis for the cluster ($\Delta t_i^{i+1} > 1$ s and $t_i > 100$ s) in Figure 2 yields $\Delta t_i^{i+1} \approx 0.13^{+0.18}_{-0.08}\ t_i^{0.81\pm0.11}$. We note the surprising consistency of this phenomenology to that reported for 1E 2259 + 586 (see Figure 10 of Gavriil et al. 2004). Finally, there is no significant dependence of burst fluence with event and waiting time in log–log (coefficient of determination $r^2 \approx 0.1$ and 0.02, respectively) for the cluster highlighted in Figure 2. Thus, for the bulk of events, the statistics of FRB events in FRB 121102 bear striking similarity to magnetar short bursts.

Gourdji et al. (2019) also remark on lognormality of waiting times in a collection of FRB 121102 Arecibo bursts, but that

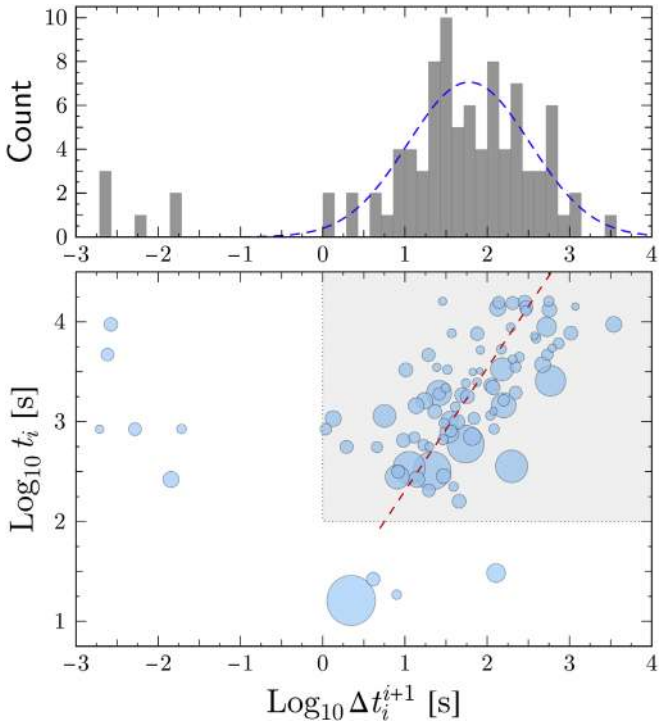

Figure 2. (Bottom) Next burst waiting time Δt_i^{i+1} vs. arrival time t_i for FRB 121102 (Z18). The area of circles is proportional to fluence. For the boxed cluster, a power law $\Delta t_i^{i+1} = 0.13\, t_i^{0.81}$ is represented by the dashed red line. (Top) Histogram of $\log_{10}\Delta t_i^{i+1}$. The dashed blue curve illustrates a lognormal distribution with mean 60 s and width 0.74 dex.

sample is insufficient to establish the power-law relation as in Figure 2.

Figure 2, which was constructed as an analog to Figure 10 of Gavriil et al. (2004), may be understood as follows. The arrival times exhibit approximately a loguniform distribution for the event density (number of events in time interval dt) $N(t)dt \propto dt/t = d\log t$ for the boxed region of Figure 2 (this nonstationary Poissonian character was noted by Z18 but not its form). The coarse-grained loguniform nature of arrival times is depicted in Figure 3, which is a reduction of the highlighted region in the bottom panel of Figure 2 onto the vertical axis. KS/AD tests do not reject this description. Formally, the arrival times can then be regarded as an "order statistic" of random variables from a continuous loguniform distribution. The log character implies scale invariance (suggestive of multiplicative physical processes with memory) and signifies that the relative ratios of arrival times, rather than offset to an arbitrarily assumed zero time, is what is relevant. The "power-law relation" in Figure 2, which simply captures the gross trend of increasing waiting time with arrival time, is an empirical construct whose origin can be traced to the arrival time loguniformity. The fit exponent of this relation is contingent of the dynamic range of the timescales during a burst storm, and would clearly be very poorly constrained if the dynamic range of timescales were small. Conversely, the fit exponent approaches unity (from below) for a large dynamic range of timescales where loguniformity is realized, i.e., when the indicated range with arrows in Figure 3 is more extensive.

Under the assumption that the arrival times are an order statistic of random variables drawn from a loguniform distribution, the waiting time distribution is humped. This hump flattens and asymptotes to loguniformity for infinite

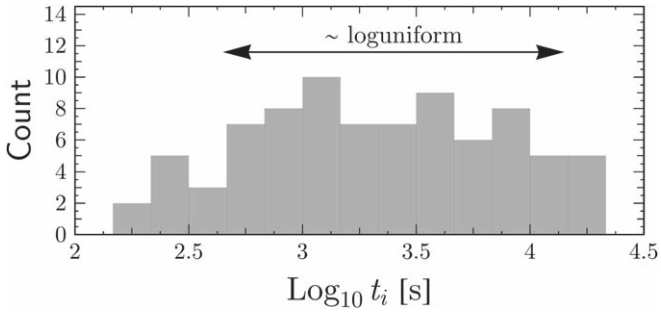

Figure 3. Coarse-grained loguniformity of arrival times for the cluster of events highlighted in the bottom panel of Figure 2.

episode duration. The lognormal distribution (parabola in log–log) is a low-order nontrivial approximation for a humped distribution at the peak. The number of events and truncated sampling (i.e., the dynamic range of timescales in Figure 3) of the $\propto 1/t$ event density governs the mean and width of the distribution—this phenomenology may be regulated by physics that sets the characteristic duration of burst episodes to hours/days and the number of bursts in the tens or hundreds. Hence, the similarity of FRB 121102 and magnetar short burst phenomenology is fundamentally linked by the $1/t$ (or loguniformity) event density underpinning burst triggering during episodes, and by the comparable characteristic lifespan of such burst storms. This fundamental similarity is one aspect which motivates our model in Section 3.

The six short-waiting-time events in Figure 2, if not spurious, may reflect double-peaked events below instrumental threshold—such short-waiting-time events are also encountered in studies of magnetar short bursts. As will become apparent in due course, we ascribe a different physical origin for these events in our model than events which follow the gross trend in Figure 2.

2.2. PA Stability during and between Bursts

FRB 121102 exhibits ∼100% linear polarization in its pulses. Of the 16 Arecibo/GBT bursts reported in Michilli et al. (2018), 13 have measured polarization angles (PAs), and exhibit a sample mean of $\langle \mathrm{PA}\rangle \sim 63°$ and standard deviation $\sigma_{\mathrm{PA}} \sim 8°$, i.e., a relatively narrow range of PAs. For this sample, KS and AD tests disfavor ($p < 0.05$) a bracketed uniform distribution $\mathrm{PA} \in [\langle \mathrm{PA}\rangle - \chi, \langle \mathrm{PA}\rangle + \chi]$ for range $\chi \gtrsim 40°$, suggesting total chaos ($\chi = 90°$) is improbable. Similarly, for the 13 PA measurements (out of 21 GBT bursts), Gajjar et al. (2018) report $\langle \mathrm{PA}\rangle \sim 77°$ with standard deviation $\sigma_{\mathrm{PA}} \sim 7°$ with $\chi \gtrsim 30°$ disfavored by KS/AD tests. The modestly different sample means $\langle \mathrm{PA}\rangle$ of the two data sets may reflect the dissimilar sampling cadences.

Both Michilli et al. (2018) and Gajjar et al. (2018) reported that during bursts, the PA was fixed to within ∼5°–10°. As noted by Michilli et al. (2018), this is suggestive of an emission process where the observed burst duration (apart from scattering broadening) is intrinsic rather than a geometric effect of an observer intercepting a sweeping beam from a polar cap.[7] Apart from viewing geometry influences, this is a natural consequence if the phase width of the beam $\delta\phi$ is wide in

[7] In radio pulsars where radio emission arises from the polar cap open zone, the PA can sweep significantly ($\gg 5°$) during a single pulse (e.g., Everett & Weisberg 2001). This is generally true when the pulsar magnetic obliquity is appreciably nonzero.

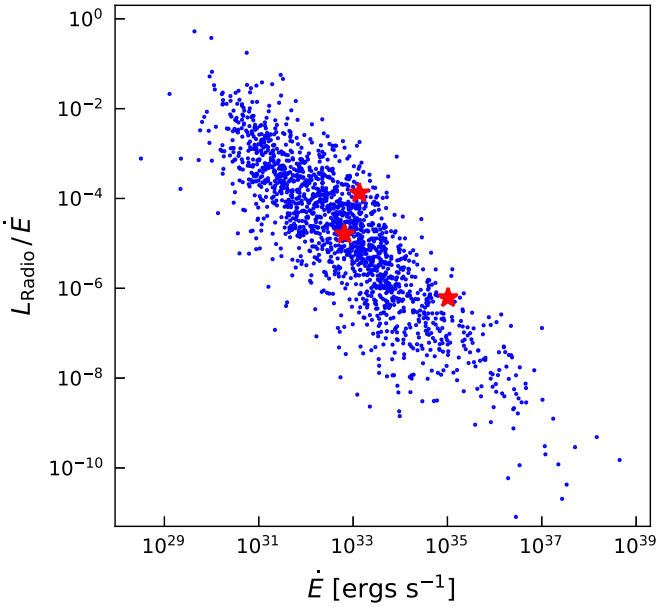

Figure 4. Observed radio efficiency of pulsars (magnetars in red) at 1.4 GHz (ATNF catalog, Manchester et al. 2005).

comparison to the ratio of the intrinsic burst duration τ to the period of the rotator P, and $\delta\phi \gg \tau/P$ where for slow rotators like magnetars $\tau/P \ll 1$. Indeed, the high rate of bursts, the null-correlation with rotational phase, and statistical similarity to magnetar short bursts suggest FRB 121102's beaming cones are broad. Then, geometry is likely the driver of PA variation between bursts.

3. The Charge-starved Magnetar Model

The striking similarity between the fluence and recurrence rate phenomenology of magnetar short bursts and FRB 121102 pulses motivates us to consider a model where repeating FRBs are generated in magnetospheres of (some) magnetars experiencing short bursts. Additional arguments in favor of such an explanation would be the fact that highly magnetized NSs—pulsars and some magnetars—do exhibit coherent radio emission and the high magnetic fields of NSs would help to explain the high polarization seen in the pulses of FRB 121102 (some other FRBs also exhibit high linear polarization e.g., Masui et al. 2015; Petroff et al. 2017; Caleb et al. 2018). Such linear polarization is suggestive of either generation in or natural eigenmode propagation within strong and ordered magnetic fields (e.g., Melrose 2017).

In order for such a model to be viable it must at least account for (i) the energetics of individual radio pulses, $\mathcal{E}_{\rm iso} \sim 10^{37}$–$10^{39}$ erg, (ii) their short duration, $\lesssim$1 ms, and (iii) explain why such coherent high intensity burst-like radio emission is not seen from known magnetars during bursts or perhaps at other epochs. Here we address these items and develop a schematic model for repeating FRBs generated by magnetars.

In Figure 4 we display the ratio of radio luminosity to spindown power for pulsars, and three known anomalous X-ray pulsars (AXPs) observed to emit pulsed radio signals sporadically.[8] It is evident from this plot that the pulsar emission mechanism(s) could operate with the efficiency in the range of 10^{-2}–10^{-6} in physical conditions present in NS magnetospheres, converting Poynting flux into coherent radio emission; attempts to correct for beaming empirically (Arzoumanian et al. 2002) may further relax this efficiency constraint, especially for pulsars near the death band (i.e., charge starvation). The leading model for magnetar short bursts invoke deformations of the NS crust. For magnetoelastic deformations, a characteristic energy scale of 10^{42}–10^{43} erg is plausibly attainable (e.g., Thompson & Duncan 2001; Perna & Pons 2011; Lander et al. 2015). The quasithermal short burst energies up to $\sim 10^{42}$ erg are then calorimetric for the event energy release into the magnetosphere. For FRB 121102, a pulsar-like emission mechanism converting $\sim 10^{-4}$–10^{-2} of the total energy released into the magnetosphere may comfortably account for the energetics of radio bursts without invoking beaming; such efficiency is, at least, not inconsistent with estimated efficiencies of pulsar emission mechanisms, shown in Figure 4.

Although the specifics of the emission mechanism(s) are unknown, it is generally accepted that in most pulsars coherent radio emission is generated along open magnetic field lines at low altitudes. The critical ingredient for this mechanism is the presence of cascade zones where particles are accelerated to high energies in vacuum-like gaps. These particles emit high energy γ-rays which give rise to copious electron/positron pair cascades via magnetic pair production. In the process of such highly nonstationary plasma outflow, coherent radio emission is putatively generated. The basis for the existence of particle acceleration zones is the repeated depletion in some magnetospheric locales of charge carriers, which are transported into the pulsar wind, and the resulting inability of these regions to sustain current densities demanded by the magnetosphere. As the particle number density drops below the value necessary to support the current and charge densities required by the global magnetospheric configuration, a quasivacuum gap with high electric field appears (e.g., Timokhin 2010; Timokhin & Arons 2013). The characteristic charge density $\rho_{\rm GJ}$ needed to screen the accelerating electric field is the Goldreich–Julian charge density (Goldreich & Julian 1969), the critical current density $j_{\rm m}$ varies over the polar cap, but for most pulsars is in the range $|\boldsymbol{j}_{\rm m}| \lesssim (1\text{–}2)\rho_{\rm GJ}\, c$. In the closed field line zone, plasma is trapped. In a rotation-powered pulsar, no currents flow along closed field lines and plasma there, once generated, may be persistent, subjected only to slow diffusion-like processes, thus hindering the formation of acceleration zones and the generation of coherent emission. In the de-facto standard magnetar model (Thompson et al. 2002; Beloborodov & Thompson 2007) the magnetic field has a global twist which demands persistent "simmering" pair creation to support current flow along closed magnetic flux tubes. Plasma does flow along those field lines but is constantly replenished by low-intensity pair formation.

In a magnetar short burst, $\sim$1% of the NS surface area participates in the energy release ($T_{\rm hot}$ component, e.g., Israel et al. 2008; Lin et al. 2012; van der Horst et al. 2012), which is much larger than the polar cap area.[9] Therefore, in magnetar crustal slips, most of the energy release will involve the closed magnetic flux tubes. During such events, an electric field will be generated owing to dislocation of magnetic FPs. If the plasma density proximate to this active region is sufficient to

[8] We adopted values for radio flux at 1.4 GHz multiplied by the square of the pulsar distance in units of [mJy kpc^2] (quantity `R_Lum14` in ATNF catalog) and calculated the luminosity as $L_{\rm Radio} = 9.5 \times 10^{16} \times 4\pi$ `R_Lum14` $\Delta\nu$ [erg s^{-1}] with $\Delta\nu = 1$ GHz.

[9] The polar cap is only a small fraction of the total NS surface area, $\pi r_{\rm pc}^2/(4\pi R_*^2) \simeq 5 \times 10^{-5} P^{-1}$ with P in seconds.

screen this electric field, no pulsar-like emission mechanism may operate. Indeed, if charges are abundant, the characteristic size of regions with unscreened electric fields is of the order of the Debye length, and particles will not be accelerated to energies high enough to initiate strong cascades, e.g., Beloborodov & Thompson (2007). However, if the plasma density in the closed flux tube is below the Goldreich–Julian density associated with the burst event,[10] e.g., due to low initial field twist, then magnetospheric regions linked to this active area may become charge starved, which will lead to intense particle acceleration, pair creation, and generation of coherent radio emission via a putative pulsar-like mechanism. In this case, a larger area would emit more coherent radio emission than in pulsars/magnetars, where the emission is limited by the open zone.

Let us now estimate the critical twist of closed dipolar magnetic field lines which would allow the operation of a pulsar-like mechanism. The current density needed to support a persistent field line twist is (Beloborodov & Thompson 2007)

$$j_{\rm twist} = \frac{c}{4\pi}|\boldsymbol{\nabla}\times\boldsymbol{B}| \sim \frac{c}{4\pi}\frac{B}{R_*}\sin^2\theta_0\,\Delta\phi, \tag{2}$$

where B is the local magnetic field, θ_0 is the FP colatitude, and $\Delta\phi$ is the twist angle. The corresponding charge density is of order $\rho_{\rm twist} \sim j_{\rm twist}/c$.

Wiggling of magnetic FPs with the speed v will result in an electric field

$$E \sim \frac{v}{c}B \sim \frac{2\pi\nu\xi}{c}B, \tag{3}$$

where ν and ξ are the frequency and amplitude of oscillations, respectively. The requisite charge density to screen the accelerating electric field E in the active region provoked by wiggling of magnetic FPs may be estimated as

$$\rho_{\rm burst} \sim \frac{1}{4\pi}\frac{E}{\lambda} \sim \frac{1}{2}\frac{\xi}{\lambda}\frac{\nu}{c}B, \tag{4}$$

where λ is the characteristic wavelength of oscillations. When

$$\rho_{\rm burst} > \max\{\rho_{\rm twist}, \rho_{\rm GJ}\}, \tag{5}$$

the charge density is insufficient to screen E prompted by the NS crust motion and the resulting charge starvation would give rise to intense particle acceleration and, according our assumptions, an FRB. The charge density due to the twist is larger than the corotational Goldreich–Julian one $\rho_{\rm GJ} \sim B/(cP)$ providing $\Delta\phi \gtrsim 4\pi R_*/(cP\sin^2\theta_0) \sim 4\times10^{-5}(P/10\ {\rm s})^{-1}\sin^{-2}\theta_0$, and so we neglect $\rho_{\rm GJ}$ here onwards. Influences of corotation on the twisted currents are only relevant for altitudes much larger than considered here (Thompson et al. 2002).

From Equations (2)–(5), we obtain the limit on the preexisting local twist of magnetic field lines which allow a pulsar-like emission mechanism to operate in the closed zone,

$$\Delta\phi \lesssim \frac{2\pi R_*}{c}\nu\frac{1}{\sin^2\theta_0}\frac{\xi}{\lambda} \simeq 0.003\ \nu_{\rm kHz}\ \sigma_{-3}. \tag{6}$$

The last step in the inequality assumes that the colatitude of magnetic field FPs $\theta_0 \simeq 15^\circ$ (corresponding to flux tube filling times of $\sim$1 ms—see below); $\nu_{\rm kHz}$ is the oscillation frequency in kHz, and the strain $\sigma \equiv \xi/\lambda$ is normalized to 10^{-3}, $\sigma_{-3} \equiv 10^{-3}(\xi/\lambda)$, following usual assumptions about properties of magnetar crusts (e.g., Thompson & Duncan 1995). Equation (6) may be applied to a single dislocation of duration Δt as well, by $\nu \to 1/\Delta t$. For crustal breakage events, the strain will be larger than that for oscillations, hence, a crustal failure event may generate intense pair cascades in magnetars with larger initial twist. The limiting twist Equation (6) for typical parameters associated with magnetar bursts is lower than usually needed for persistent nonthermal emission in active magnetars (e.g., Baring & Harding 2007; Beloborodov & Thompson 2007; Beloborodov 2013a) and confirms the basic expectations of our model. Note that Equation (6) is independent of B.

The maximum potential drop which may be generated by crustal displacements is of the order of $\Delta\Phi_{\rm max} \sim E\lambda$, for E given by Equation (3). The upper limit on the energy of primary electrons accelerated by a parallel electric field above the active region would be

$$\gamma_{\rm max} \sim \frac{e\Delta\Phi_{\rm max}}{m_e c^2} \sim 10^9\ \nu_{\rm kHz}\ \sigma_{-3}\ \lambda_4^2\ B_{14}, \tag{7}$$

where m_e and e are electron mass and charge, and $\lambda_4 \equiv \lambda/10^4$ cm—the characteristic wavelengths of oscillations/displacement are normalized to 1% of the NS radius. It is evident that for any reasonable values of parameters, in the case of charge starvation, primary particles will achieve energies sufficient to trigger pair cascades. In our model, particle acceleration commences at the beginning of a short burst when burst-induced photon densities are low. Then, particle Compton drag can only arise by scattering soft thermal X-ray photons from the NS surface. The acceleration rate of a primary $\dot{\gamma}_e \sim e/(m_e c)E \sim 10^{15.5}B_{14}\nu_{\rm kHz}\sigma_{-3}\lambda_4\ {\rm s}^{-1}$ (B_{14} is the magnetic field in units of 10^{14} G) is much greater than even the peak ($\sim10^9$–$10^{12}\ {\rm s}^{-1}$) of the resonant Compton[11] cooling rate in a surface thermal photon bath (see Figures 4–6 in Baring et al. 2011); hence, the primary will accelerate until curvature losses dominate at $\gamma_e \gtrsim 10^6$. The existence of persistent polar cap coherent radio emission in some magnetars (e.g., Kramer et al. 2007) also provides strong evidence that such Compton drag is not a showstopper.

Regardless of the actual radio emission mechanism, the radio waves ought to decouple from the magnetosphere and escape to infinity to be observable. This is involved, and ultimately hinges on the dielectric tensor and anisotropic plasma dispersion relations in the strongly magnetized quantum plasma.[12] Among other factors, such as the direction of wave propagation with respect to local $\boldsymbol{B}$, the unknown local plasma distribution function and bulk Lorentz factor in the NS frame can influence cutoffs, with higher transparency for larger bulk motions. Conservatively, the plasma frequency ν_e (with zero

[10] I.e., the charge density necessary to screen E precipitated by magnetic FP dislocations.

[11] In magnetars, resonant Compton scattering is the dominant energy loss mechanism for electrons at modest Lorentz factors at low altitudes.

[12] In strong magnetic fields, vacuum polarization may dominate the dielectric tensor for wave propagation. However, its impact strongly weakens for lower energy photons. For radio photons, it can be shown that the characteristic pair number density below which vacuum birefringence dominates over plasma effects (the vacuum resonance condition e.g., Lai & Ho 2002), is far lower than even $\rho_{\rm GJ}$ for any reasonable plasma bulk Lorentz factor.

bulk motion) for the plasma supporting the twist of the closed field lines sets the characteristic wave frequency scale, below which radio emission is likely damped or anomalous,

$$\nu_e \sim \frac{1}{2\pi}\sqrt{\frac{4\pi e \rho_{\rm twist}}{m_e}} \sim \frac{1}{2\pi}\sqrt{\frac{eB}{m_e R_*}}\,\sin\theta_0\,\Delta\phi^{1/2} \qquad (8)$$

adopting Equation (2). For the limiting twist Equation (6), a limit on the plasma frequency is

$$\nu_e \lesssim \frac{1}{\sqrt{2\pi}}\omega_B^{1/2}\,\sigma^{1/2}\,\nu_{\rm osc}^{1/2} \sim 17\,B_{14}^{1/2}\,\sigma_{-3}^{1/2}\,\nu_{\rm osc,kHz}^{1/2}\quad {\rm GHz}, \qquad (9)$$

where $\omega_B = eB/(m_e c)$. Radio waves of frequencies $\nu_{\rm em} \sim 1$ GHz (in the source frame) may escape from the low-twist magnetosphere beginning at about altitudes $r_{\rm em}$ where magnetic field drops below $B_{14} \lesssim (1/17)^2$, for $r_{\rm em} \gtrsim 7\,R_* B_{0,14}^{1/3}$, where $B_{0,14}$ is the surface magnetic field (normalized to 10^{14} G). Dipolar magnetic flux tubes can extend up to maximum altitude $r_{\rm max} \simeq R_* \sin^2\theta_0$—from the limit $r_{\rm em} \gtrsim 7R_*$ for 1 GHz propagation, we obtain a restriction on the FP colatitude $\theta_{0,\rm em} \lesssim \arcsin(\sqrt{R_*/r_{\rm em}}) \simeq 23^\circ$. For twists smaller than the critical one, the range of magnetic field lines along which the emission can escape is larger, as follows from Equation (8). Note that Equation (9) in some sense may be regarded as a radius-to-frequency mapping (e.g., Cordes 1978).

Above, we examined limits on the emission height considering the transparency of plasma generated by the persistent twist of magnetic field lines, without considering the transparency of plasma that generates radio emission. This plasma, generated in the event leading to the FRB, ought to be much denser than the background plasma through which the radio emission propagates, but also relativistic. Then, the altitude of transparency may be larger than that estimated above, and the colatitudes of magnetic field lines FPs may be smaller than $\theta_{0,\rm em}$. However, details of the putative pulsar-like emission mechanism are poorly understood, and the straightforward arguments used above might not be applicable to the emission regions above the active zone. Moreover, as in pulsars, field curvature is expected to play a role in transparency. Hence, the estimates for the extent of the regions from which the GHz radio emission can escape based on the background plasma density represent an upper limit on the size of those regions.

In our scenario, the pulsar-like mechanism may operate only until the dense pair plasma fills the closed flux tube originating in the active zone. Then, even if the motion of field line FPs persists on longer timescales, plasma density will remain high, and particle acceleration and the associated coherent emission will be stifled. The time needed to supply charges for a flux tube extending up to the maximum distance $r_{\rm max}$ will be of the order of $\tau \sim 2r_{\rm max}/c$. For the dipolar field, the FP colatitude for the flux tube which will be populated by plasma in $\tau \lesssim 1$ ms is $\theta_{0,1\ {\rm ms}} \gtrsim 14^\circ$.

The clearing of flux tubes permeated by plasma from pair cascades is not immediate. If these field lines were twist-free, the plasma may persist a long time, subject to slow diffusion-like processes, and hinder subsequent FRBs if the same FP is dislocated. If those field loops are mildly twisted, clearing can proceed faster as charged particles will be exhausted for supporting current flowing along these field lines due their twist. The minimum time required for clearing of the flux tube of length $\ell_B \sim 2r_{\rm max}$ of pair plasma can be estimated as $\sim \ell_B\,\kappa\rho_{\rm burst}/j_{\rm twist}$, where κ is the multiplicity of the pair cascade. For the case of near-threshold twists, when $\rho_{\rm burst} \sim \rho_{\rm twist}$, the minimum interval between bursts would be κ times longer than the burst duration. For expected values $\kappa \sim 10^2$–10^3 (e.g., Timokhin & Harding 2019) the minimum interval between successive bursts would be 0.1–1 s. In our model, lower twists would be associated with longer minimum recurrence times.

If magnetoelastic torsional oscillations follow the initial slippage event, as observed in some magnetar short bursts, multiple FP dislocation events could occur. The period of crustal torsional oscillations, $1/\nu_{\rm osc} \sim (50\text{–}300\ {\rm Hz})^{-1}$, is generally shorter than the twist charge depletion timescale $\ell_B\kappa\rho_{\rm burst}/j_{\rm twist}$. However, for oscillations with large amplitude, the radio emission mechanism can operate for larger persistent twists. The cascade multiplicity dependency on the amplitude is expected to be rather weak (e.g., Timokhin & Harding 2019), hence, the larger current caused by larger twist would lead to faster clearing of flux tubes. Then, multiple nonstationary pair avalanches and radio bursts may transpire during such torsional oscillations. Since core–crust coupling is known to damp such oscillations on a timescale of $\sim$0.2–2 s (Levin 2006; Huppenkothen et al. 2014b; Miller et al. 2019), the duration and number of such time-clustered events ought be limited to a few events in $\sim$2 s time intervals, or up to when the oscillation amplitude ξ is too small to initiate pair cascades and satisfy Equation (5). Furthermore, because of such damping and charge loading, the FRB pulse fluences may be lower for events spawned in oscillations than the initial pulses triggered in conditions of higher charge starvation. These expectations are in general agreement with short-waiting-time events in Figure 2. Speculatively, millisecond timescale substructures within longer bursts (e.g., Hessels et al. 2019; CHIME/FRB Collaboration et al. 2019) might also arise from plasma blobs spawned by crustal oscillations.

High linear polarization of individual bursts can be naturally explained in the framework of our model. There are two orthogonal eigenmodes of propagation in a magnetized plasma, with one generally dominant (e.g., Melrose & Stoneham 1977; Melrose 1979). Lu et al. (2019) recently argued that in magnetar magnetospheres, the dominant X-mode can enter the so-called "adiabatic walking" regime (e.g., Cheng & Ruderman 1979; Wang et al. 2010) when propagation induces high linear polarization and the PA traces the geometry of the inner magnetosphere. They estimated the freeze-out radius $r_{\rm fo}$, where radio emission finally decouples from plasma, preserving the acquired linear polarization, for the corotation plasma density. Here we estimate $r_{\rm fo}$ for much higher plasma density required by the twisted magnetosphere. Adopting Equation (18) from Lu et al. (2019) and substituting expressions for the charge density through Equation (2) and the threshold on the twist of magnetic field lines Equation (7), for $\nu_{\rm em} \sim 1$ GHz radio waves, the freeze-out radius is

$$\frac{r_{\rm fo}}{R_*} \lesssim 18\,B_{0,14}^{1/3}\,R_{B,7}^{1/3}\,a_{0,5}^{-1/3}\,\nu_{\rm em,GHz}^{-1/3}\,\sigma_{-3}^{1/3}\,\nu_{\rm osc,kHz}^{1/3}, \qquad (10)$$

where $R_B \sim 10^7 R_{B,7}$ cm is the radius of the curvature of the field lines, $a_0 \sim 10^5 a_{0,5} \gg 1$ is the characteristic nonlinearity parameter, which may be regarded as the induced electron Lorentz factor $a_0 \sim e\,E_R/(\omega m_e c) \lesssim 10^5$–$10^7$ by the high-intensity radio

pulse of angular frequency ω. Here $E_R \sim \sqrt{\mathcal{E}_{\rm iso}/R_*^3}$ is the characteristic electric field of the radio pulse. From Equation (10) it is clear that adiabaticity may be attained in large zones of the magnetospheres. The freeze-out radius is generally larger than the radius above which 1 GHz radio emission is transparent, $r_{\rm em} \gtrsim 7R_*$ estimated above, so the radio waves can acquire high linear polarization prior to vacuum propagation.

Periodicity in the PA variation ought to be a viable check for the model, particularly in repeating FRBs with high linear polarization. In the canonical rotating vector model (RVM; Radhakrishnan & Cooke 1969) for a static dipole, for viewing angle $\zeta \in (0, \pi)$ and magnetic obliquity $\alpha \in (0, \pi/2)$ with respect to the spin axis, the allowed parameter space for which the PA has bounded $<180^\circ$ variation is $0 < \beta/2 < \pi/2 - \alpha$, where $\beta = \zeta - \alpha$ is the impact parameter. Under these assumptions for RVM, it may be shown that $2\chi' \equiv {\rm PA}_{\rm max} - PA_{\rm min}$ is restricted to $\chi' \geqslant \alpha$. Hence, in our model $\alpha \lesssim 40^\circ$ (see Section 2.2); this result obtained under the assumption of no preferential sampling of spin phases in bursts, is in contrast with the lighthouse effect in pulsars. If there exist spin phases where radio emission is either unobservable or not amenable to the coherent radio process, then gaps in the folded PA sweeps may manifest; however, such gaps would imprint periodicity in arrival times. The null-detection of periodicity in arrival times of FRB 121102 pulses suggests such beaming selection effects may be small/inconsequential and the pulses ought to sample any spin phase of the rotator, similar to magnetar short bursts.

4. Summary and Outlook

In this paper, motivated by the remarkable similarity between statistics of magnetar short bursts and FRB 121102, we suggest that some FRBs originate from magnetars with low magnetospheric twist. Short bursts in such magnetars would give rise to pulsar-like radio emission mechanisms along closed field lines linked to the active region powering the burst. The crucial component of our model is that the plasma density above the active region powering the magnetar burst is insufficient to screen the accelerating electric field induced by the dislocation of magnetic FPs following crustal slippage events. Moreover, in magnetars with high twist, plasma density in the closed field line zone would be too high to allow $\sim$1 GHz radio transparency from most of the closed field line region. Hence, for self-consistency, this mechanism can operate only in magnetars which cannot support high plasma densities in the closed field line zone; this sets an upper bound on the global twist. Such an object could be an aged magnetar which lost most of its twist by the decay of internal toroidal fields, a high-B pulsar undergoing magnetar-like activity or a younger magnetar in a mode of low twist. The low twist can account for the absence of FRBs from Galactic magnetars, which are believed to have larger twists than the limit in this work, not only because of charge starvation during crustal dislocations, but also because of absorption of radio pulses in the closed zone. Based on the empirical data about pulsar radio emission efficiency, we assume a 10^{-4}–10^{-2} fraction of the calorimetric short burst energy can be released in form of FRB, which is ample to account for observed fluences in FRB 121102.

The proposed mechanism might not work well for magnetar giant flares (which is consistent with nondetection of radio bursts in the 2004 giant flare of SGR 1806–20, Tendulkar et al. 2016). The energy release in giant flares is much larger ($\sim 10^{44}$–10^{46} erg) and the spectral character is distinct (spectra extending to much higher photon energies) from short bursts (e.g., Woods & Thompson 2006). Giant flares should arise from a qualitatively different physical origin than short bursts (e.g., Thompson & Duncan 2001; van Putten et al. 2016) possibly involving reconnection in a large magnetospheric volume with large twists (e.g., Parfrey et al. 2012, 2013). During giant flares, huge amounts of dense pair plasma is generated, but the pair cascades that produce this plasma may be quite different from those that might lead to coherent radio emission. Pair formation may be distributed over a large volume, and the leading process may be two-photon pair creation, i.e., such cascades might not involve fast screening of large sustained (on FRB timescales) electric fields in charge starved regions by newly generated plasma, that are presumed to be at the core of pulsar-like emission mechanisms. So, even at the very onset of a giant flare, conditions might be unfavorable for the generation of coherent radio bursts. Moreover, once dense plasma and photon fields are generated, they will suppress any further production of nonthermal particle populations and/or will be opaque for radio emission.

The event rate of cosmological FRBs will clearly depend on the operating longevity of the progenitor. If the low-twist FRB mode is the next stage in the life of a typical magnetar, then the absence of FRBs in the Galactic magnetar population sets a lower bound on the age of FRB progenitors to be $\gtrsim$3–10 kyr (SNR ages; see Beniamini et al. 2019), though such a mode may not be long-lived (or prolific), given that field decay also may act on similar timescales and predicted crustal event rates decline strongly with age (e.g., Viganò et al. 2013; Beniamini et al. 2019). Yet, the progenitor may be a young magnetar in a state of low twist. Magnetars with large-scale twists might temporarily lose their twist on a timescale of $\sim 10^2$–10^3 days (e.g., Younes et al. 2017; Coti Zelati et al. 2018), suggesting that the FRB mode with low twist may be a substantial fraction of an active magnetar's lifespan. Models of large-scale slow untwisting in magnetars (Beloborodov 2009, 2013b; Chen & Beloborodov 2017) predict a significant colatitudinal dependence to the local twist, with equatorial FPs less twisted than polar ones, and the low-twist equatorial cavity expanding with time. Then, small dispersive delays, secularly decreasing at the untwisting timescale but dependent on rotational phase, may be imprinted on pulses.

In Galactic magnetars, the timescale of damping of crustal oscillations due to core–crust coupling has been inferred to be $\sim$0.2–2 s (Huppenkothen et al. 2014b; Miller et al. 2019). This, along with the time to clear a flux tube of charges, limits the number of potential FRB recurrences in $\sim$0.2–2 s time intervals, if associated with a single active region. In such short-waiting-time event clusters (or within substructures of longer bursts), quasiperiodicity associated with the crustal torsional oscillations may become apparent in arrival times for large samples. Scrutiny of the time variation in the PA of bursts, particularly those with high linear polarization, could be also pivotal. A periodicity of order $\sim$1–10 s in the PA variation, tracing the magnetic field structure as in the RVM, will be a "smoking gun" of the pair-starved magnetar model (also see Lu et al. 2019).

The high-energy nondetection by Scholz et al. (2017) for FRB 121102 with a burst energy limit of $\lesssim 10^{45}$–10^{47} erg is

consistent with the short burst picture (since short burst energies are smaller by a factor $\ll 10^{-2}$). Photon splitting and magnetic pair production in the magnetosphere will suppress signals above a few MeV (Hu et al. 2019; Wadiasingh et al. 2019), suggesting lower energy observations would be more promising. Time coincidence *Fermi*-GBM and *Gehrels/Swift*-BAT scrutiny of future nearby FRBs might provide a stringent test of the model.

We thank Matthew G. Baring, Alice K. Harding, Jason Hessels, Demos Kazanas, Chryssa Kouveliotou, and George Younes for helpful discussions and valuable feedback on this manuscript. We also thank the anonymous referee for constructive feedback. Z.W. is supported by the NASA postdoctoral program. A.T. is supported by the NSF grant 1616632 and *Chandra* Guest Investigator program TM8-19005. This work has made use of the NASA Astrophysics Data System.

ORCID iDs

Zorawar Wadiasingh https://orcid.org/0000-0002-9249-0515
Andrey Timokhin https://orcid.org/0000-0002-0067-1272

References

Archibald, R. F., Burgay, M., Lyutikov, M., et al. 2017, ApJL, 849, L20
Arzoumanian, Z., Chernoff, D. F., & Cordes, J. M. 2002, ApJ, 568, 289
Baring, M. G., & Harding, A. K. 2007, Ap&SS, 308, 109
Baring, M. G., Wadiasingh, Z., & Gonthier, P. L. 2011, ApJ, 733, 61
Beloborodov, A. M. 2009, ApJ, 703, 1044
Beloborodov, A. M. 2013a, ApJ, 762, 13
Beloborodov, A. M. 2013b, ApJ, 777, 114
Beloborodov, A. M. 2017, ApJL, 843, L26
Beloborodov, A. M., & Thompson, C. 2007, ApJ, 657, 967
Beniamini, P., Hotokezaka, K., van der Horst, A., & Kouveliotou, C. 2019, MNRAS, 487, 1426
Caleb, M., Keane, E. F., van Straten, W., et al. 2018, MNRAS, 478, 2046
Camilo, F., Ransom, S. M., Halpern, J. P., et al. 2006, Natur, 442, 892
Camilo, F., Scholz, P., Serylak, M., et al. 2018, ApJ, 856, 180
Chen, A. Y., & Beloborodov, A. M. 2017, ApJ, 844, 133
Cheng, A. F., & Ruderman, M. A. 1979, ApJ, 229, 348
Cheng, B., Epstein, R. I., Guyer, R. A., & Young, A. C. 1996, Natur, 382, 518
CHIME/FRB Collaboration, Amiri, M., Bandura, K., et al. 2019, Natur, 566, 235
Collazzi, A. C., Kouveliotou, C., van der Horst, A. J., et al. 2015, ApJS, 218, 11
Cordes, J. M. 1978, ApJ, 222, 1006
Coti Zelati, F., Rea, N., Pons, J. A., Campana, S., & Esposito, P. 2018, MNRAS, 474, 961
Elenbaas, C., Watts, A. L., & Huppenkothen, D. 2018, MNRAS, 476, 1271
Everett, J. E., & Weisberg, J. M. 2001, ApJ, 553, 341
Gajjar, V., Siemion, A. P. V., Price, D. C., et al. 2018, ApJ, 863, 2
Gavriil, F. P., Kaspi, V. M., & Woods, P. M. 2004, ApJ, 607, 959
Goldreich, P., & Julian, W. H. 1969, ApJ, 157, 869
Gourdji, K., Michilli, D., Spitler, L. G., et al. 2019, arXiv:1903.02249
Göğüş, E., Woods, P. M., Kouveliotou, C., et al. 1999, ApJL, 526, L93
Göğüş, E., Woods, P. M., Kouveliotou, C., et al. 2000, ApJL, 532, L121
Hessels, J. W. T., Spitler, L. G., Seymour, A. D., et al. 2019, ApJL, 876, L23
Hu, K., Baring, M. G., Wadiasingh, Z., & Harding, A. K. 2019, MNRAS, 486, 3327
Huppenkothen, D., D'Angelo, C., Watts, A. L., et al. 2014c, ApJ, 787, 128
Huppenkothen, D., Heil, L. M., Watts, A. L., & Göğüş, E. 2014a, ApJ, 795, 114
Huppenkothen, D., Watts, A. L., & Levin, Y. 2014b, ApJ, 793, 129
Hurley, K. J., McBreen, B., Rabbette, M., & Steel, S. 1994, A&A, 288L, L49
Israel, G. L., Romano, P., Mangano, V., et al. 2008, ApJ, 685, 1114
Katz, J. I. 2016, ApJ, 826, 226
Katz, J. I. 2018, PrPNP, 103, 1
Katz, J. I. 2019, MNRAS, 487, 491
Kramer, M., Stappers, B. W., Jessner, A., Lyne, A. G., & Jordan, C. A. 2007, MNRAS, 377, 107
Lai, D., & Ho, W. C. G. 2002, ApJ, 566, 373
Lander, S. K., Andersson, N., Antonopoulou, D., & Watts, A. L. 2015, MNRAS, 449, 2047
Levin, Y. 2006, MNRAS, 368, L35
Lin, L., Göğüş, E., Baring, M. G., et al. 2012, ApJ, 756, 54
Linscott, I. R., & Erkes, J. W. 1980, ApJL, 236, L109
Lu, W., Kumar, P., & Narayan, R. 2019, MNRAS, 483, 359
Lyubarsky, Y. 2014, MNRAS, 442, L9
Lyutikov, M. 2017, ApJL, 838, L13
Lyutikov, M. 2019, arXiv:1901.03260
Manchester, R. N., Hobbs, G. B., Teoh, A., & Hobbs, M. 2005, AJ, 129, 1993
Masui, K., Lin, H.-H., Sievers, J., et al. 2015, Natur, 528, 523
Melrose, D. B. 1979, AuJPh, 32, 61
Melrose, D. B. 2017, RvMPP, 1, 5
Melrose, D. B., & Stoneham, R. J. 1977, PASAu, 3, 120
Metzger, B. D., Margalit, B., & Sironi, L. 2019, MNRAS, 485, 4091
Michilli, D., Seymour, A., Hessels, J. W. T., et al. 2018, Natur, 553, 182
Miller, M. C., Chirenti, C., & Strohmayer, T. E. 2019, ApJ, 871, 95
Parfrey, K., Beloborodov, A. M., & Hui, L. 2012, ApJL, 754, L12
Parfrey, K., Beloborodov, A. M., & Hui, L. 2013, ApJ, 774, 92
Perna, R., & Pons, J. A. 2011, ApJ, 727, L51
Petroff, E., Burke-Spolaor, S., Keane, E. F., et al. 2017, MNRAS, 469, 4465
Petroff, E., Hessels, J. W. T., & Lorimer, D. R. 2019, A&ARv, 27, 4
Platts, E., Weltman, A., Walters, A., et al. 2018, arXiv:1810.05836
Popov, S. B., & Postnov, K. A. 2010, in Evolution of Cosmic Objects through their Physical Activity, ed. H. A. Harutyunian, A. M. Mickaelian, & Y. Terzian (Yerevan: NAS RA), 129
Popov, S. B., & Postnov, K. A. 2013, arXiv:1307.4924
Radhakrishnan, V., & Cooke, D. J. 1969, ApL, 3, 225
Savchenko, V., Neronov, A., Beckmann, V., Produit, N., & Walter, R. 2010, A&A, 510, A77
Scholz, P., Bogdanov, S., Hessels, J. W. T., et al. 2017, ApJ, 846, 80
Spitler, L. G., Scholz, P., Hessels, J. W. T., et al. 2016, Natur, 531, 202
Tendulkar, S. P., Bassa, C. G., Cordes, J. M., et al. 2017, ApJL, 834, L7
Tendulkar, S. P., Kaspi, V. M., & Patel, C. 2016, ApJ, 827, 59
Thompson, C., & Duncan, R. C. 1995, MNRAS, 275, 255
Thompson, C., & Duncan, R. C. 2001, ApJ, 561, 980
Thompson, C., Lyutikov, M., & Kulkarni, S. R. 2002, ApJ, 574, 332
Timokhin, A. N. 2010, MNRAS, 408, 2092
Timokhin, A. N., & Arons, J. 2013, MNRAS, 429, 20
Timokhin, A. N., & Harding, A. K. 2019, ApJ, 871, 12
Turolla, R., Zane, S., & Watts, A. L. 2015, RPPh, 78, 116901
van der Horst, A. J., Kouveliotou, C., Gorgone, N. M., et al. 2012, ApJ, 749, 122
van Putten, T., Watts, A. L., Baring, M. G., & Wijers, R. A. M. J. 2016, MNRAS, 461, 877
Viganò, D., Rea, N., Pons, J. A., et al. 2013, MNRAS, 434, 123
Wadiasingh, Z., Younes, G., Baring, M. G., et al. 2019, arXiv:1903.05648
Wang, C., Lai, D., & Han, J. 2010, MNRAS, 403, 569
Wang, W., Luo, R., Yue, H., et al. 2018, ApJ, 852, 140
Woods, P. M., & Thompson, C. 2006, in Soft Gamma Repeaters and Anomalous X-ray Pulsars: Magnetar Candidates, ed. W. H. G. Lewin & M. van der Klis (Cambridge: Cambridge Univ. Press), 547
Younes, G., Kouveliotou, C., Jaodand, A., et al. 2017, ApJ, 847, 85
Younes, G., Kouveliotou, C., van der Horst, A. J., et al. 2014, ApJ, 785, 52
Zhang, Y. G., Gajjar, V., Foster, G., et al. 2018, ApJ, 866, 149